Published in final edited form as:
Arch Ophthalmol. 2006 June ; 124(6): 827–836.

Ultrahigh-Resolution Optical Coherence Tomography of Surgically Closed Macular Holes

Tony H. Ko, PhD, **Andre J. Witkin, BS**, **James G. Fujimoto, PhD**, **Annie Chan, BS**, **Adam H. Rogers, MD**, **Caroline R. Baumal, MD**, **Joel S. Schuman, MD**, **Wolfgang Drexler, PhD**, **Elias Reichel, MD**, and **Jay S. Duker, MD**

Department of Electrical Engineering and Computer Science and Research Laboratory of Electronics, Massachusetts Institute of Technology, Cambridge, Mass (Drs Ko and Fujimoto); New England Eye Center, Tufts–New England Medical Center, Tufts University, Boston, Mass (Mr Witkin, Ms Chan, and Drs Rogers, Baumal, Reichel, and Duker); University of Pittsburgh Medical Center Eye Center, Department of Ophthalmology, University of Pittsburgh School of Medicine, Pittsburgh, Pa (Dr Schuman); and Christian Doppler Laboratory, Center for Biomedical Engineering and Physics, Medical University Vienna, Vienna, Austria (Dr Drexler).

Abstract

Objective— To evaluate retinal anatomy using ultrahigh-resolution optical coherence tomography (OCT) in eyes after successful surgical repair of full-thickness macular hole.

Methods— Twenty-two eyes of 22 patients were diagnosed as having macular hole, underwent pars plana vitrectomy, and had flat/closed macular anatomy after surgery, as confirmed with biomicroscopic and OCT examination findings. An ultrahigh-resolution–OCT system developed for retinal imaging, with the capability to achieve approximately 3-μm axial resolution, was used to evaluate retinal anatomy after hole repair.

Results— Despite successful closure of the macular hole, all 22 eyes had macular abnormalities on ultrahigh-resolution–OCT images after surgery. These abnormalities were separated into the following 5 categories: (1) outer foveal defects in 14 eyes (64%), (2) persistent foveal detachment in 4 (18%), (3) moderately reflective foveal lesions in 12 (55%), (4) epiretinal membranes in 14 (64%), and (5) nerve fiber layer defects in 3 (14%).

Conclusions— With improved visualization of fine retinal architectural features, ultrahigh-resolution OCT can visualize persistent retinal abnormalities despite anatomically successful macular hole surgery. Outer foveal hyporeflective disruptions of the junction between the inner and outer segments of the photoreceptors likely represent areas of foveal photoreceptor degeneration. Moderately reflective lesions likely represent glial cell proliferation at the site of hole reapproximation. Thin epiretinal membranes do not seem to decrease visual acuity and may play a role in reestablishing foveal anatomy after surgery.

Since the introduction of vitrectomy for the treatment of macular hole in 1991, vitreous surgery has become the standard in therapy for the disease.[1] The procedure has undergone numerous

Correspondence: Jay S. Duker, MD, New England Eye Center, Tufts–New England Medical Center, 750 Washington St, Boston, MA 02111 (JDuker@tufts-nemc.org).

Author Contributions: Dr Duker had full access to all the data in the study and takes responsibility for the integrity of the data and the accuracy of the data analysis.

Previous Presentation: This paper was presented in part at the 2005 Annual Meeting of Association for Research in Vision and Ophthalmology; May 1–5, 2005; Fort Lauderdale, Fla.

Financial Disclosure: Drs Fujimoto and Schuman receive royalties from intellectual property licensed by the Massachusetts Institute of Technology to Carl Zeiss Meditec and receive research support from Carl Zeiss Meditec. Dr Drexler is a consultant for Carl Zeiss Meditec.

improvements with increasing success rates. Success has been defined in terms of anatomical closure and improvement of visual acuity. With the addition of internal limiting membrane (ILM) peeling to the surgical procedure, recent anatomical closure rates of 85% to 100% and visual acuity improvement rates of 85% to 95% have been reported.[2–6] Although functional success is fairly simple to assess via best-corrected visual acuity (BCVA), anatomical success is more difficult to define. In 1998, Tornambe et al[7] defined the following 3 surgical end points based on fundus examination that have since been widely accepted: elevated/open, flat/open, and flat/closed. These anatomical end points correlated with visual acuity after surgery.

Optical coherence tomography (OCT) was originally demonstrated in 1991 as a unique biomedical imaging tool capable of cross-sectional imaging at 10-μm axial resolution in tissue.[8] Optical coherence tomography was first demonstrated for in vivo human retinal imaging in 1995, and the first reports describing OCT imaging of macular holes were published by Hee et al[9,10] and Puliafito et al[11] in the same year. With OCT, it has become much easier to define and understand the retinal anatomy before and after macular hole surgery. In addition to assessment of postsurgical retinal status, OCT has helped to determine the time frame of resolution to normal retinal anatomy after surgery, and has also helped to explain poor visual acuity in cases where the retina appeared normal on results of biomicroscopic examination.[12–21]

Poor visual acuity after surgery is understandable in patients with persistently open macular holes (surgical failures); however, poor visual acuity has also been noted in patients with clinically closed holes. Recently, reports have been published showing an abnormality of the photoreceptors on OCT in patients with otherwise normal foveal anatomy after macular hole surgery. The OCT abnormality was a disruption of the line representing the junction between the inner and outer segments of the photoreceptors (IS/OS junction), identical to what Kitaya et al[18] and Hikichi et al[19] termed the *photoreceptor reflection*, and correlated with a poorer visual acuity[20] and a larger preoperative macular hole diameter.[21] This finding is confirmed by previous histopathologic studies,[22–24] which showed photoreceptor degeneration and glial proliferation in both presurgical and postsurgical macular holes. Visual distortion after macular hole surgery has also been attributed to epiretinal membrane (ERM) formation. Two cases were related by Uemoto et al,[25] in which ERMs were visualized on OCT after undergoing ILM peeling during vitrectomy for macular hole repair. Finally, the effect of ILM peeling on the adjacent nerve fiber layer (NFL) remains unclear.

Our group has recently developed a new generation of ultrahigh-resolution (UHR)–OCT technology that significantly improves the axial image resolution of OCT.[26,27] Using a state-of-the-art femtosecond laser as the light source for OCT imaging, this new technology achieves axial image resolutions of approximately 3 μm in the human eye, compared with approximately 10 μm by standard-resolution OCT. The enhanced imaging capabilities of UHR-OCT improve the visualization of fine intraretinal architectural morphology such as the ganglion cell layer, photoreceptor layers, and retinal pigment epithelium (RPE).[28] In a previous report from our group,[29] a comparison between standard-resolution OCT and UHR-OCT of macular holes found that UHR-OCT improved the visualization of hole architecture, particularly the changes in photoreceptor morphology associated with macular hole formation and repair.

In this study, we examine UHR-OCT images from a series of 22 eyes of 22 patients who had flat/closed anatomy as defined by Tornambe et al[7] after a standard vitrectomy procedure for macular hole repair. In select cases, we compare standard-resolution OCT images (obtained on STRATUSOCT; Carl Zeiss Meditec Inc, Dublin, Calif) with UHR-OCT images. We postulate that UHR-OCT imaging will demonstrate abnormalities in retinal architecture with greater detail after hole repair, particularly at the level of the photoreceptors.

METHODS

Optical coherence tomography is analogous to ultrasonography, except that OCT uses light instead of sound. The principle of OCT has been explained in detail in previous publications.[8,9,11] The axial resolution in OCT is inversely proportional to the bandwidth of the light source used for imaging. Standard-resolution OCT uses a superluminescent diode light source that generates approximately 25 nm of bandwidth at an approximately 800-nm center wavelength and is capable of axial resolution of approximately 10 μm. Standard-resolution OCT images have approximately 10-μm axial and 20-μm transverse resolution in tissue and consist of 1024 axial pixels and 512 transverse pixels (total, 524 288 pixels). Standard-resolution OCT images of the macula use standard scans of 2-mm axial depth and 6 mm in the transverse direction.

Our group developed a prototype UHR-OCT system capable of performing studies in the ophthalmology clinic.[29] For this UHR-OCT system, a specially designed titanium:sapphire femtosecond laser was used as the light source for imaging.[30] This laser generates approximately 125 nm of bandwidth at an approximately 815-nm center wavelength, and the UHR-OCT system is capable of achieving axial resolution of approximately 3 μm. The UHR-OCT images have approximately 3-μm axial and 15- to 20-μm transverse resolution in tissue and consist of 3000 axial and 600 transverse pixels (total, 1 800 000 pixels). The UHR-OCT images use scans with a 1.5-mm axial depth that span 6 mm in the transverse direction. The prototype UHR-OCT clinical ophthalmic system has been described in detail in a previous study comparing standard-resolution OCT and UHR-OCT images of macular holes.[29] A UHR-OCT image of a normal eye is shown in Figure 1. Optical coherence tomography is performed within well-established safe retinal exposure limits set by the American National Standards Institute,[31] and the UHR-OCT prototype uses the same incident optical power as standard-resolution OCT does for imaging.

The standard-resolution OCT protocol was followed on both OCT systems to enable a direct comparison of the resulting images. Six radial macular scans 6 mm in length each were acquired at angles separated by 30° intervals. After OCT was completed, all UHR-OCT images were corrected for axial motion using standard reregistration algorithms. These algorithms have been used in all of the previous prototype and commercial OCT systems.[32] The standard-resolution OCT images are usually not corrected for axial motion because the commercial software exports only uncorrected raw images. Because the standard-resolution OCT can acquire an image in approximately 1.3 seconds compared with approximately 4 seconds for the UHR-OCT system, the axial motions in the standard-resolution OCT images are usually not significant; however, we have also developed software to correct the raw standard-resolution OCT images in cases where axial motion is substantial.

Imaging was performed using the commercially available standard-resolution OCT and our UHR-OCT prototype in the ophthalmology clinic of the New England Eye Center at Tufts–New England Medical Center. The study was approved by the institutional review board committees of Tufts–New England Medical Center and the Massachusetts Institute of Technology and complies with the Health Insurance Portability and Accountability Act of 1996. Written informed consent was obtained from all subjects in this study before UHR-OCT was performed.

Twenty-two eyes of 22 patients were diagnosed as having stage 2, 3, or 4 macular hole according to the Gass classification system, and subsequently underwent anatomically successful vitrectomy surgery.[33,34] Full-thickness macular hole was diagnosed after complete preoperative ophthalmologic examination, including intraocular pressure measurement, lens clarity evaluation, refraction, axial length measurement, and biomicroscopic examination of the fovea and vitreous. The BCVA was measured using standard Snellen eye charts. Standard-

resolution OCT was used to confirm the macular hole status. In 1 case, a macular hole was diagnosed as stage 1a by results of a fundus examination, but standard-resolution OCT showed it was a stage 2 hole. Patients with macular pathology other than macular hole were excluded from this study.

The patients all underwent pars plana vitrectomy between September 1, 2002, and December 31, 2004. Surgery was performed at Tufts–New England Medical Center by 1 of 4 attending ophthalmologists (A.H.R., C.R.B., E.R., and J.S.D.). Nineteen (86%) of 22 eyes underwent peeling of the ILM. Two of these eyes underwent staining of the ILM with indocyanine green intraoperatively. During surgery, peripheral retinal tears and/or lattice degeneration were noted in 7 patients (32%). Cryopexy was performed in 3 of these patients, and laser retinopexy was performed in the other 4 patients. All patients underwent air/fluid exchange. Injection of 15% perfluoropropane gas (3 patients [14%]) or 20%, 25%, or 30% sulfur hexafluoride gas (19 patients [86%]) was then performed. Phacoemulsification of a nuclear sclerotic cataract with placement of a posterior chamber intraocular lens was jointly performed in 1 patient. Surgery times ranged from 40 to 90 minutes.

After surgery, strict face-down positioning was ordered for 7 to 10 days. Follow-up examinations were performed at 1 day, 1 week, and 1, 2, 6, and 12 months after operation. The BCVA was measured, and biomicroscopic examination and standard-resolution OCT were performed at all postoperative visits. All patients included in this study had flat/closed macular holes after surgery, as confirmed by biomicroscopy and standard-resolution OCT. All patients underwent UHR-OCT at various postoperative intervals (mean, 3.2 months; range, 0.5–14 months), although 1 patient underwent UHR-OCT more than 6 months after surgery (14 months). Six of 22 eyes also underwent UHR-OCT on a second postoperative follow-up visit (mean, 8.5 months; range, 2–18 months). Foveal thickness was not measured in this study because foveal thickness has shown only moderate correlation with visual acuity in several previous studies with larger patient numbers.[13,17,20,35,36]

RESULTS

Of the 22 patients, 6 were men and 16 were women, with a median age of 64.2 years at the time of diagnosis (age range, 51–77 years). Preoperative visual acuity ranged from 20/40 to 2/200, with a mean of 20/158. According to the Gass classification system,[33,34] 13 eyes (59%) had stage 2, 7 (32%) had stage 3, and 2 (9%) had stage 4 holes. All 22 patients underwent preoperative standard-resolution OCT, and 17 underwent preoperative UHR-OCT.

At the time of the first postoperative UHR-OCT, visual acuities ranged from 20/25 to 4/200, with a mean of 20/110. Eight of 22 patients had a BCVA of 20/200 or worse at that time. The first postoperative UHR-OCT was performed from 2 weeks to 1 month later in 7 patients, from 1 to 6 months later in 14 patients, and after 6 months (ie, 14 months later) in 1 patient. Six patients had a second postoperative UHR-OCT image obtained between 2 and 18 months after surgery. In the time between the first and second postoperative UHR-OCT in these 6 patients, BCVA had improved in 3.

Abnormalities in retinal anatomy were observed on UHR-OCT images in all 22 patients (100%) after macular hole repair. These retinal abnormalities were further divided into the following 5 categories: outer foveal hyporeflective defects, persistent foveal detachment, moderately reflective foveal lesions, ERMs, and NFL defects.

Fourteen (64%) of 22 patients demonstrated hyporeflective defects in the outer fovea. The mean BCVA for this group was 20/78 after surgery. The outer foveal defects were a small, hyporeflective disruption in the normally hyperreflective IS/OS junction (Figure 2) or an outer foveal cystic space (Figure 3). Another 4 patients (18%) had small areas of persistent foveal

detachment that elevated the foveal photoreceptor segments off the RPE (Figure 4A–D) but did not change the normal foveal inner contour. Mean BCVA for this group was 20/119 after surgery. Outer foveal defects and/or detachment were persistent in all 6 patients who underwent postoperative imaging a second time, although some demonstrated a decrease in the subfoveal space or cystic area (Figure 4E–H).

The remaining 4 patients (18%) had large, moderately reflective lesions replacing all foveal retinal layers, including photoreceptors (Figure 5). Mean BCVA for this group was 20/345 after surgery. Smaller, moderately reflective lesions were also observed within the inner retinal layers of the fovea in 8 other patients (Figure 3), for a total of 12 patients with moderately reflective foveal lesions (55%). These 12 patients had a mean BCVA of 20/130 after surgery.

Epiretinal membranes were observed in the postoperative UHR-OCT images for 14 (64%) of 22 patients. Mean BCVA for this group was 20/108 after surgery. Epiretinal membrane on an UHR-OCT image was defined as a thin, highly reflective line immediately above the sensory retina (Figures 3, 4, and 6). Epiretinal membranes were observed in patients with and without intraoperative ILM peeling.

Finally, postoperative NFL defects were observed on UHR-OCT images in 3 (14%) of 22 patients. Mean BCVA in this group was 20/91 after surgery. All 3 patients with NFL defects underwent ILM peeling during macular hole surgery, with no intraoperative indocyanine green staining. The NFL defects in these patients might have been caused by ILM peeling during macular hole surgery because the corresponding preoperative UHR-OCT images for these patients showed normal NFL anatomy (Figure 6).

In addition, because of the superior resolution of UHROCT, a separate highly reflective layer was visualized between the photoreceptor IS/OS junction and RPE layers (red asterisk, Figures 1, 3, and 4). This layer can be seen in healthy eyes, as well as those with macular holes. In patients with outer foveal cystic spaces, this middle layer was disrupted in areas corresponding to disruptions of the IS/OS junction (Figure 3). In patients with persistent foveal detachments, this middle layer was lifted away from the RPE, along with the photoreceptor IS/OS junction (Figure 4G and H). The reflective layer between the IS/OS and the RPE could be clearly visualized in 17 (77%) of the 22 patients, but this layer was not always visualized in all 6 radial UHROCT images for the same subject.

COMMENT

Ultrahigh-resolution OCT was able to demonstrate the following 5 different retinal abnormalities after macular hole surgery: outer foveal hyporeflective defects, persistent foveal detachment, moderately reflective foveal lesions, ERMs, and NFL defects. Foveal photoreceptor abnormalities were consistent findings in all patients. Previously, histopathologic studies of unrepaired and repaired macular holes have also shown photoreceptor atrophy.[22–24,37] A study by Guyer et al[23] of 22 full-thickness holes not treated surgically showed photoreceptor degeneration in all patients for a mean distance of 480 μm from the hole margins. In 2 other reports,[24,37] 3 eyes were studied histopathologically after macular hole surgery. In these patients, Müller cells and/or astrocytes replaced photoreceptors at the site of hole reapproximation; the external limiting membrane was also disrupted at the fovea.

Four published reports[18–21] studied photoreceptor abnormalities using standard-resolution OCT after macular hole surgery. These reports also showed a disruption in the highly reflective line above the RPE representing the photoreceptor IS/OS junction, or what Kitaya et al[18] and Hikichi et al[19] termed the *photoreceptor reflection.* The reports by Kitaya et al[18] and Villate et al[20] also showed a correlation between photoreceptor disruption and decreased

postoperative visual acuity. In our study, unlike the previous OCT studies, we reported photoreceptor abnormalities in all the patients undergoing postoperative imaging. This higher incidence is likely due to the increased resolution of UHR-OCT, which has previously been shown to enhance visualization of smaller photoreceptor abnormalities that are not seen on standard-resolution OCT images.[28,29]

Twelve (55%) of 22 patients had a moderately reflective foveal lesion on UHR-OCT images after macular hole repair. This finding most likely represents a glial cell proliferative response, which has been shown to occur histopathologically at the foveal defect after macular hole repair.[22–24,37] Four patients had larger areas of foveal reflectivity, which effectively replaced all the intraretinal layers of the fovea (Figure 5), whereas the remaining 8 patients had smaller lesions of moderate reflectivity within the inner foveal layers.

Fourteen (64%) of 22 patients had ERMs on UHROCT images after macular hole surgery. The high percentage of ERM formation is not surprising. An essential part of macular hole surgery is the creation of a posterior vitreous detachment that is a known cause of ERM formation. Only minimal histopathologic information about surgically repaired macular holes is available; therefore, it is difficult to correlate our data with known histopathologic findings.[24,37] The histopathologic report by Guyer et al[23] showed an ERM in 16 (73%) of 22 full-thickness macular holes, which is consistent with our data. However, in our study, most of the patients underwent peeling of the ILM intraoperatively. Another report by Uemoto et al[25] shows an epimacular proliferative response on OCT in 2 (5%) of 44 patients after ILM peeling for idiopathic macular holes.

The larger percentage of patients with ERMs in our study is likely owing to the higher axial resolution of UHROCT compared with standard-resolution OCT. Most of the ERMs in this study may have been thinner than 10 μm, the minimum resolution of standard-resolution OCT. Thin ERMs are unlikely to affect vision negatively and may play a role in macular hole closure after surgery. High anatomical closure rates have been shown after ILM peeling, and it has been suggested that this is owing to stimulation of glial and Müller cell proliferation, which may aid in sealing the hole.[2–6]

Another possibility is that these detected ERMs are actually ILM. With the increased resolution of UHR-OCT, the ILM might become visible, particularly after surgery where peeling of the ILM has been attempted. However, Foos[38] has reported average ILM thicknesses of approximately 2.5 μm in histology of the posterior retina, less than the axial resolution of UHR-OCT, so we find this explanation less likely.

Three (14%) of 22 patients had localized NFL defects in UHR-OCT images acquired after macular hole surgery. Because all 3 patients with postoperative NFL defects underwent ILM peeling during surgery, NFL damage in these patients may have been caused by intraoperative ILM peeling. Alternatively, NFL damage may have been due to elevations in postoperative intraocular pressures. The NFL damage likely occurred during or after macular hole surgery because the corresponding preoperative UHR-OCT images for these patients show normal NFL anatomy. Because the numbers are small, no conclusions can be made about the potential of ILM peeling on damaging the NFL structure; however, it is reassuring that even with the higher resolution of UHR-OCT, frank NFL defects were seen in only a small percentage of patients. In addition, the 3 patients with postoperative NFL defects all showed visual improvement after macular hole surgery. Therefore, it is not known whether the postoperative NFL defects affected the visual outcome for these patients.

Another finding on UHR-OCT images in this study was the visualization of a previously unidentified retinal layer between the photoreceptor IS/OS junction and the RPE. The actual anatomical correlate of the layers within the complex of the photoreceptor outer segment and

the RPE on UHR-OCT images has been disputed.[27,28,39–41] However, we have labeled the IS/OS junction and RPE layers in this report according to the most common interpretation.[29,39] Disruption of the unidentified reflective layer in corresponding areas of IS/OS disruption in these macular hole cases suggests that this layer is part of the neural retina (Figure 3). It may represent a reflection created by photoreceptor-RPE interdigitation, or a reflection from the photoreceptor outer segment terminals. Ultrahigh-resolution–OCT with subsequent histological analysis of retinal tissue in various types of retinal pathology would be necessary to definitively identify this reflective OCT layer.

The limitations of the current study include the variety of surgical techniques used for full-thickness macular hole repair, the limited number of patients included in this study, and the need for axial motion correction in the UHR-OCT images. However, regardless of the surgical technique used, retinal and photoreceptor abnormalities were seen in all patients, indicating that some photoreceptor disruption resulting from a full-thickness macular hole generally persists even after surgical reapproximation. Epiretinal membranes were detected regardless of whether ILM peeling was performed. In the future, more rapid OCT techniques will eliminate the need for motion correction in UHR-OCT and possibly provide more definitive and quantitative visualization of these retinal abnormalities.[42]

CONCLUSIONS

We performed an imaging study of surgically closed macular holes using an UHR-OCT system. Ultrahigh-resolution OCT was able to demonstrate the following 5 different retinal abnormalities after macular hole surgery: outer foveal hyporeflective defects, persistent foveal detachments, foveal lesions of moderate reflectivity, ERMs, and NFL defects. Foveal photoreceptor defects suggest residual abnormalities in photoreceptor cells after macular hole repair. Foveal lesions of moderate reflectivity likely represent a glial cell proliferative response that replaces normal foveal anatomy at the region of retinal reapproximation after macular hole surgery. Epiretinal membranes were detected with UHR-OCT in most of our patients and may be a common occurrence after macular hole surgery. Nerve fiber layer defects may have been a result of ILM peeling during macular hole surgery. The results from this study demonstrate the ability to detect higher frequencies of these abnormalities on UHR-OCT images compared with previous OCT reports. The enhanced ability of UHR-OCT to visualize small retinal defects can be used to improve the understanding of macular hole pathogenesis and the tracking of hole closures after vitreous surgery.

Acknowledgements

Funding/Support: This study was supported in part by contracts R01-EY11289-16, R01-EY13178, and P30-EY13078 from the National Institutes of Health; contracts ECS-0119452, FWF P14218-PSY, FWF Y159-PAT, and CRAF-1999-70549 from the National Science Foundation; contract F49620-98-1-0139 from the Air Force Office of Scientific Research; contract F49620-01-1-0186 from Medical Free Electron Laser Program; and Carl Zeiss Meditec.

References

1. Kelly NE, Wendel RT. Vitreous surgery for idiopathic macular holes: results of a pilot study. Arch Ophthalmol 1991;109:654–659. [PubMed: 2025167]
2. Brooks HL Jr. Macular hole surgery with and without internal limiting membrane peeling. Ophthalmology 2000;107:1939–1949. [PubMed: 11013203]
3. Mester V, Kuhn F. Internal limiting membrane removal in the management of full-thickness macular holes. Am J Ophthalmol 2000;129:769–777. [PubMed: 10926987]
4. Smiddy WE, Feuer W, Cordahi G. Internal limiting membrane peeling in macular hole surgery. Ophthalmology 2001;108:1471–1478. [PubMed: 11470703]

5. Benson WE, Cruickshanks KC, Fong DS, et al. Surgical management of macular holes: a report by the American Academy of Ophthalmology. Ophthalmology 2001;108:1328–1335. [PubMed: 11425696]
6. Haritoglou C, Gass CA, Schaumberger M, Gandorfer A, Ulbig MW, Kampik A. Long-term follow-up after macular hole surgery with internal limiting membrane peeling. Am J Ophthalmol 2002;134:661–666. [PubMed: 12429240]
7. Tornambe PE, Poliner LS, Cohen RG. Definition of macular hole surgery end points: elevated/open, flat/open, flat/closed. Retina 1998;18:286–287. [PubMed: 9654428]
8. Huang D, Swanson EA, Lin CP, et al. Optical coherence tomography. Science 1991;254:1178–1181. [PubMed: 1957169]
9. Hee MR, Izatt JA, Swanson EA, et al. Optical coherence tomography of the human retina. Arch Ophthalmol 1995;113:325–332. [PubMed: 7887846]
10. Hee MR, Puliafito CA, Wong C, et al. Optical coherence tomography of macular holes. Ophthalmology 1995;102:748–756. [PubMed: 7777274]
11. Puliafito CA, Hee MR, Lin CP, et al. Imaging of macular diseases with optical coherence tomography. Ophthalmology 1995;102:217–229. [PubMed: 7862410]
12. Jumper JM, Gallemore RP, McCuen BW II, Toth CA. Features of macular hole closure in the early postoperative period using optical coherence tomography. Retina 2000;20:232–237. [PubMed: 10872926]
13. Imai M, Iijima H, Gotoh T, Tsukahara S. Optical coherence tomography of successfully repaired idiopathic macular holes. Am J Ophthalmol 1999;128:621–627. [PubMed: 10577532]
14. Uemoto R, Yamamoto S, Aoki T, Tsukahara I, Yamamoto T, Takeuchi S. Macular configuration determined by optical coherence tomography after idiopathic macular hole surgery with or without internal limiting membrane peeling. Br J Ophthalmol 2002;86:1240–1242. [PubMed: 12386079]
15. Ip MS, Baker BJ, Duker JS, et al. Anatomical outcomes of surgery for idiopathic macular hole as determined by optical coherence tomography. Arch Ophthalmol 2002;120:29–35. [PubMed: 11786054]
16. Kang SW, Ahn K, Ham DI. Types of macular hole closure and their clinical implications. Br J Ophthalmol 2003;87:1015–1019. [PubMed: 12881347]
17. Apostolopoulos MN, Koutsandrea CN, Moschos MN, et al. Evaluation of successful macular hole surgery by optical coherence tomography and multifocal electroretinography. Am J Ophthalmol 2002;134:667–674. [PubMed: 12429241]
18. Kitaya N, Hikichi T, Kagokawa H, Takamiya A, Takahashi A, Yoshida A. Irregularity of photoreceptor layer after successful macular hole surgery prevents visual acuity improvement. Am J Ophthalmol 2004;138:308–310. [PubMed: 15289151]
19. Hikichi T, Kitaya N, Konno S, Takahashi J, Mori F, Yoshida A. Effect of preoperative detection of photoreceptor displacement on postoperative foveal findings in eyes with idiopathic macular hole. Br J Ophthalmol 2003;87:506–507. [PubMed: 12642325]
20. Villate N, Lee JE, Venkatraman A, Smiddy WE. Photoreceptor layer features in eyes with closed macular holes: optical coherence tomography findings and correlation with visual outcomes. Am J Ophthalmol 2005;139:280–289. [PubMed: 15733989]
21. Moshfeghi AA, Flynn HW Jr, Elner SG, Puliafito CA, Gass JD. Persistent outer retinal defect after successful macular hole repair. Am J Ophthalmol 2005;139:183–184. [PubMed: 15652846]
22. Frangieh GT, Green WR, Engel HM. A histopathologic study of macular cysts and holes. Retina 1981;1:311–336. [PubMed: 7348853]
23. Guyer DR, Green WR, de Bustros S, Fine SL. Histopathologic features of idiopathic macular holes and cysts. Ophthalmology 1990;97:1045–1051. [PubMed: 2402416]
24. Funata M, Wendel RT, de la Cruz Z, Green WR. Clinicopathologic study of bilateral macular holes treated with pars plana vitrectomy and gas tamponade. Retina 1992;12:289–298. [PubMed: 1485013]
25. Uemoto R, Yamamoto S, Takeuchi S. Epimacular proliferative response following internal limiting membrane peeling for idiopathic macular holes. Graefes Arch Clin Exp Ophthalmol 2004;242:177–180. [PubMed: 14648135]
26. Drexler W, Morgner U, Kartner FX, et al. In vivo ultrahigh-resolution optical coherence tomography. Opt Lett 1999;24:1221–1223.

27. Drexler W, Morgner U, Ghanta RK, Kartner FX, Schuman JS, Fujimoto JG. Ultrahigh-resolution ophthalmic optical coherence tomography. Nat Med 2001;7:502–507. [PubMed: 11283681]
28. Drexler W, Sattmann H, Hermann B, et al. Enhanced visualization of macular pathology with the use of ultrahigh-resolution optical coherence tomography. Arch Ophthalmol 2003;121:695–706. [PubMed: 12742848]
29. Ko TH, Fujimoto JG, Duker JS, et al. Comparison of ultrahigh- and standard-resolution optical coherence tomography for imaging macular hole pathology and repair. Ophthalmology 2004;111:2033–2043. [PubMed: 15522369]
30. Kowalevicz AM, Schibli TR, Kartner FX, Fujimoto JG. Ultralow-threshold Kerrlens mode-locked Ti: Al2O3 laser. Opt Lett 2002;27:2037–2039.
31. American National Standards Institute. Safe Use of Lasers. New York, NY: American National Standards Institute; 1993.
32. Swanson EA, Izatt JA, Hee MR, et al. In-vivo retinal imaging by optical coherence tomography. Opt Lett 1993;18:1864–1866.
33. Gass JD. Idiopathic senile macular hole: its early stages and pathogenesis. Arch Ophthalmol 1988;106:629–639. [PubMed: 3358729]
34. Gass JD. Reappraisal of biomicroscopic classification of stages of development of a macular hole. Am J Ophthalmol 1995;119:752–759. [PubMed: 7785690]
35. Kumagai K, Ogino N, Demizu S, et al. Variables that influence visual acuity after macular hole surgery. Jpn J Ophthalmol 2001;45:112.
36. Amari F, Ohta K, Kojima H, Yoshimura N. Predicting visual outcome after macular hole surgery using scanning laser ophthalmoscope microperimetry. Br J Ophthalmol 2001;85:96–98. [PubMed: 11133722]
37. Madreperla SA, Geiger GL, Funata M, de la Cruz Z, Green WR. Clinicopathologic correlation of a macular hole treated by cortical vitreous peeling and gas tamponade. Ophthalmology 1994;101:682–686. [PubMed: 8152763]
38. Foos RY. Vitreoretinal juncture: topographical variations. Invest Ophthalmol 1972;11:801–808. [PubMed: 4561129]
39. Anger EM, Unterhuber A, Hermann B, et al. Ultrahigh resolution optical coherence tomography of the monkey fovea: identification of retinal sublayers by correlation with semithin histology sections. Exp Eye Res 2004;78:1117–1125. [PubMed: 15109918]
40. Ahnelt PK, Drexler W. Ultrahigh resolution optical coherence tomography of the monkey fovea: identification of retinal sublayers by correlation with semithin histology sections. Exp Eye Res 2005;80:449–450.letter
41. van Velthoven ME, Verbraak FD. Ultrahigh resolution optical coherence tomography of the monkey fovea: identification of retinal sublayers by correlation with semithin histology sections. Exp Eye Res 2005;80:447–448. [PubMed: 15721627]letter
42. Wojtkowski M, Bajraszewski T, Gorczynska I, et al. Ophthalmic imaging by spectral optical coherence tomography. Am J Ophthalmol 2004;138:412–419. [PubMed: 15364223]

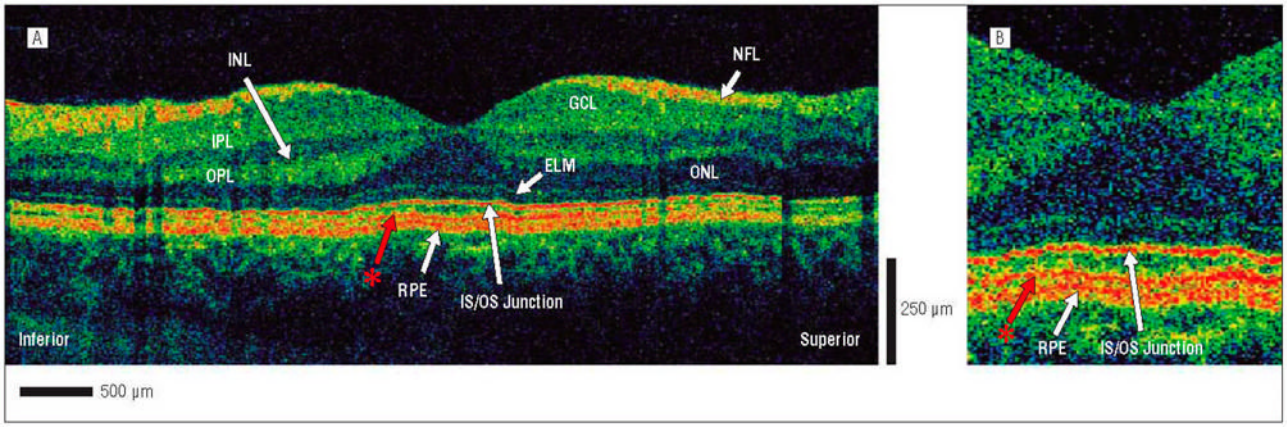

Figure 1.

Ultrahigh-resolution–optical coherence tomography (UHR-OCT) image of a normal eye. A, The following retinal layers are labeled: nerve fiber layer (NFL), ganglion cell layer (GCL), inner plexiform layer (IPL), inner nuclear layer (INL), outer plexiform layer (OPL), outer nuclear layer (ONL), external limiting membrane (ELM), junction of the photoreceptor inner and outer segments (IS/OS), and retinal pigment epithelium (RPE). The red asterisk represents a previously unidentified layer between the IS/OS junction and the RPE. B, Magnification (×2) of the UHR-OCT image showing the unidentified retinal layer (red asterisk) in more detail.

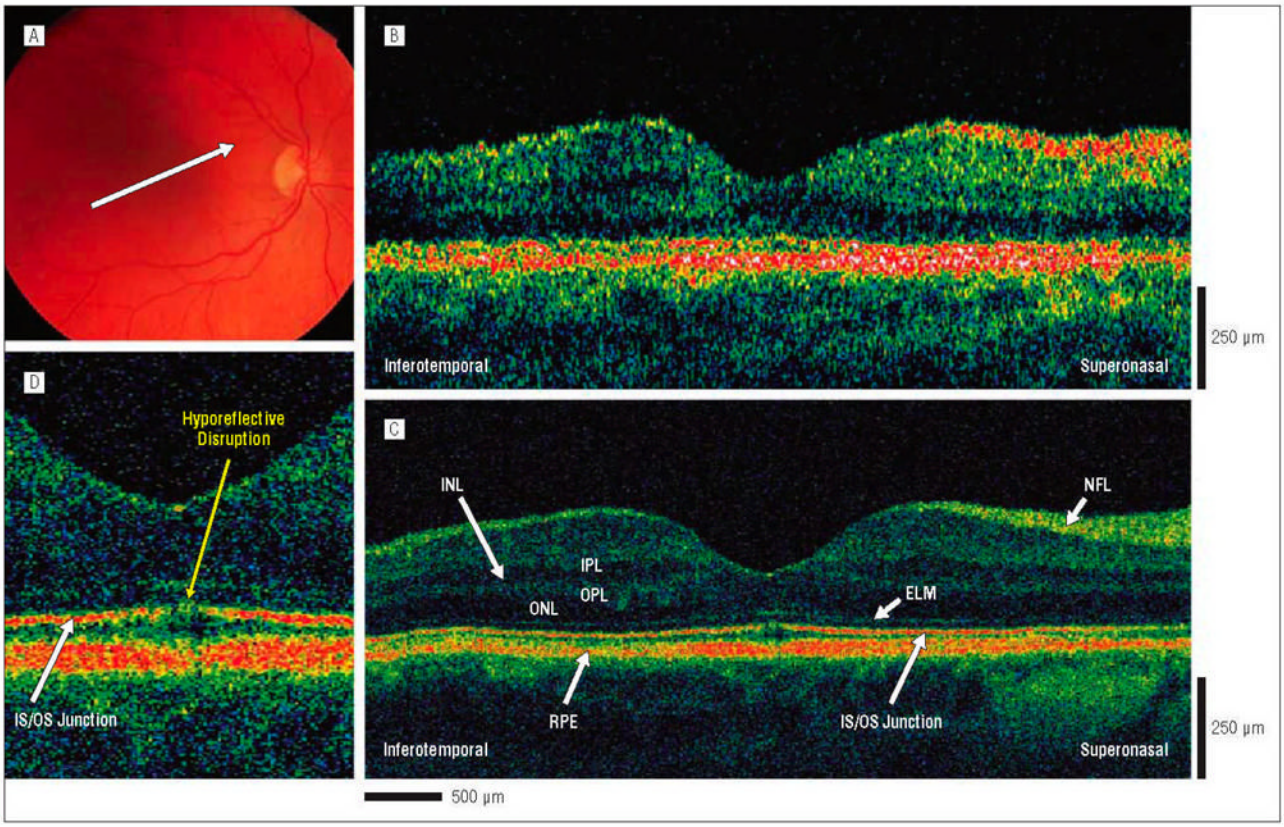

Figure 2.

Postoperative macular hole, 3 months after surgical repair. The patient is a 60-year-old woman who underwent initial evaluation for a stage 2 macular hole in the right eye and had a preoperative visual acuity of 20/80. She underwent pars plana vitrectomy with internal limiting membrane peel and injection of 20% sulfur hexafluoride gas. Three months postoperatively, the hole was flat and closed on results of examination, and visual acuity was 20/40. A, Fundus photograph showing direction of optical coherence tomography (OCT) images. B, Standard-resolution OCT image acquired in the scan direction. C, Corresponding UHR-OCT image acquired in the scan direction. The hyporeflective disruption of the foveal photoreceptor IS/OS junction is much more visible in the UHR-OCT than in the standard-resolution OCT image. D, Magnification (×2) of the UHR-OCT image. A hyporeflective disruption of the normally hyperreflective IS/OS junction is clearly visualized in the foveal outer retina. The ELM remains intact across the macula. Abbreviations are described in the legend to Figure 1.

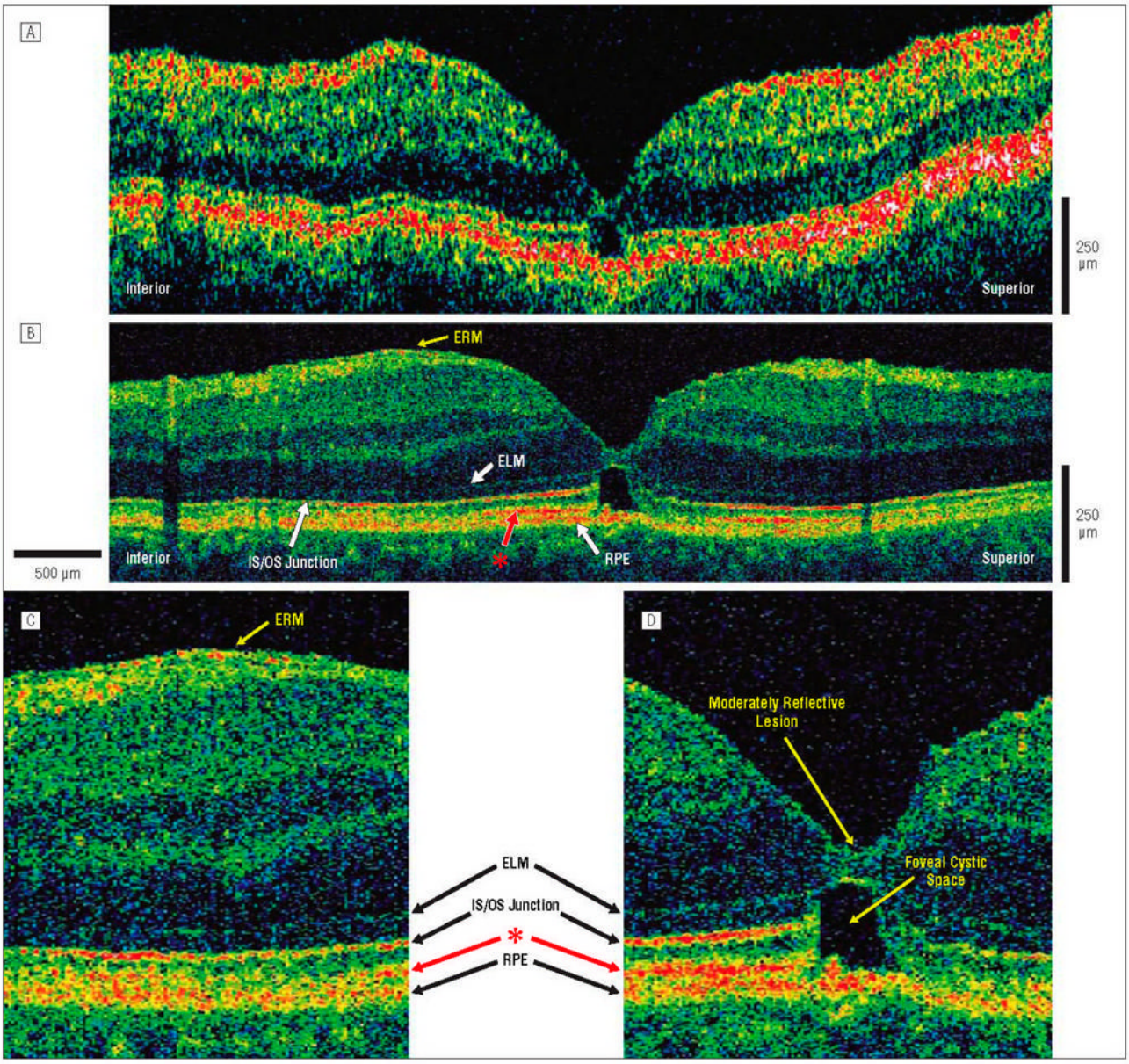

Figure 3.

Postoperative macular hole, 1.25 months after surgical repair. The patient is a 51-year-old man who underwent initial evaluation for a stage 3 macular hole in the left eye and had a preoperative visual acuity of 20/100. He underwent pars plana vitrectomy with internal limiting membrane peel and injection of 25% sulfur hexafluoride gas. One month later, the hole was flat and closed on results of examination, and visual acuity was 20/40. Optical coherence tomography (OCT) images were obtained vertically across the macula in the inferior-superior direction. A, Standard-resolution OCT image acquired in the inferior-superior direction. A hyporeflective disruption in the outer retina is clearly visualized. B, Corresponding UHR-OCT image acquired in the same scan direction. The hyporeflective disruption in the outer retina is likely to be caused by the presence of an outer foveal cystic space. A thin epiretinal membrane (ERM) is present inferior to the fovea. The hyperreflective layer (red asterisk) between the IS/OS junction and RPE appears to stop abruptly in the region of foveal cystic space, suggesting that this layer belongs to the neural retina. C, Magnification (×2) of the UHR-OCT image shows the thin,

hyperreflective ERM above the nerve fiber layer. D, Magnification (×2) of the UHR-OCT image. An outer foveal cystic space appears to be the origin of the hyporeflective disruption in the outer retina. A small moderatively reflective foveal lesion is also visualized within the inner retina. The ELM and RPE remain intact across the macula. The previously unidentified hyperreflective layer (red asterisk) present between the IS/OS junction and RPE is abruptly disrupted at the cystic space in tandem with the IS/OS junction, suggesting that this layer belongs to the neural retina. Abbreviations are described in the legend to Figure 1.

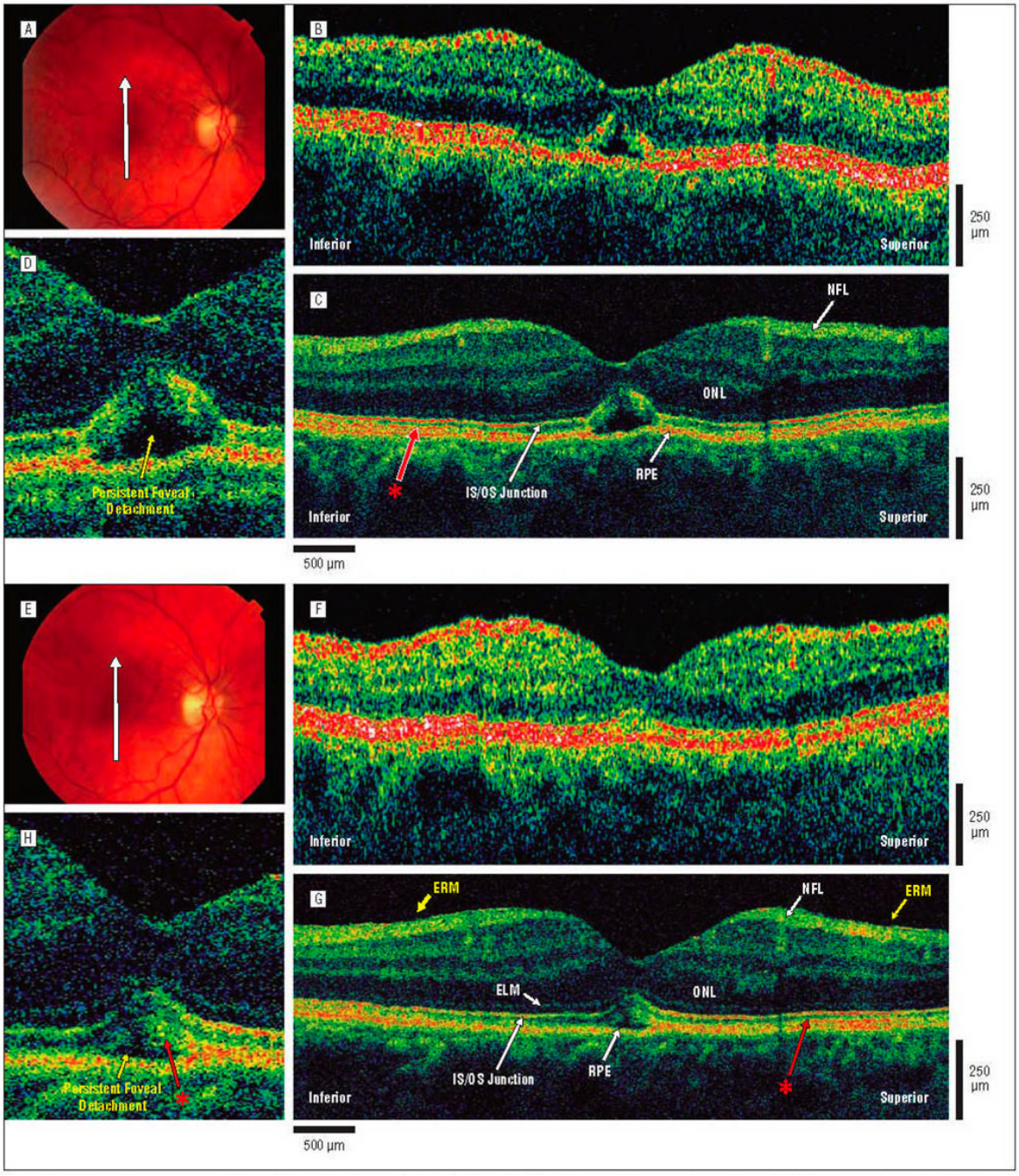

Figure 4.

Postoperative macular hole, 1 and 4.5 months after surgical repair. The patient is a 64-year-old woman who underwent initial evaluation for a stage 2 macular hole in the right eye and had a preoperative visual acuity of 20/100. She underwent pars plana vitrectomy with internal limiting membrane peel and injection of 25% sulfur hexafluoride gas. One month later, the hole was flat and closed on results of examination, and visual acuity was 20/125. At 4.5 months after surgery, the hole was flat and closed on results of examination, and visual acuity was 20/70. A, Postoperative fundus photograph obtained at 1 month shows the direction of optical coherence tomography (OCT) images. B, Standard-resolution OCT image acquired 1 month after surgical repair. A small area of persistent foveal detachment is evident. C, Corresponding

UHR-OCT image acquired 1 month after surgical repair. A previously unidentified hyperreflective layer (red asterisk) is present between the IS/OS junction and RPE. This hyperreflective layer between the IS/OS junction and RPE is visualized in the peripheral macula, but is not apparent in the foveal region near the elevated outer retina. D, Magnification (×2) of the UHR-OCT image. Persistent foveal detachment is present, with lifting of the photoreceptor IS/OS junction away from the RPE. E, Postoperative fundus photograph obtained at 4.5 months shows the same direction of OCT scans as those acquired at 1 month. F, Standard-resolution OCT image acquired 4.5 months after surgical repair. A small disruption of the IS/OS junction may be present at the fovea. G, Corresponding UHR-OCT image acquired 4.5 months after surgical repair. A thin epiretinal membrane (ERM) is visualized inferior and superior to the fovea. The hyperreflective layer (red asterisk) between the IS/OS junction and RPE layers appears to extend closer to the foveal region. H, Magnification (×2) of the UHR-OCT image. The persistent foveal detachment appears to be resolving, but the IS/OS junction remains slightly lifted away from the RPE with the hyperreflective layer (red asterisk) appearing to also follow the IS/OS junction away from the RPE. The RPE remains intact across the macula. Abbreviations are described in the legend to Figure 1.

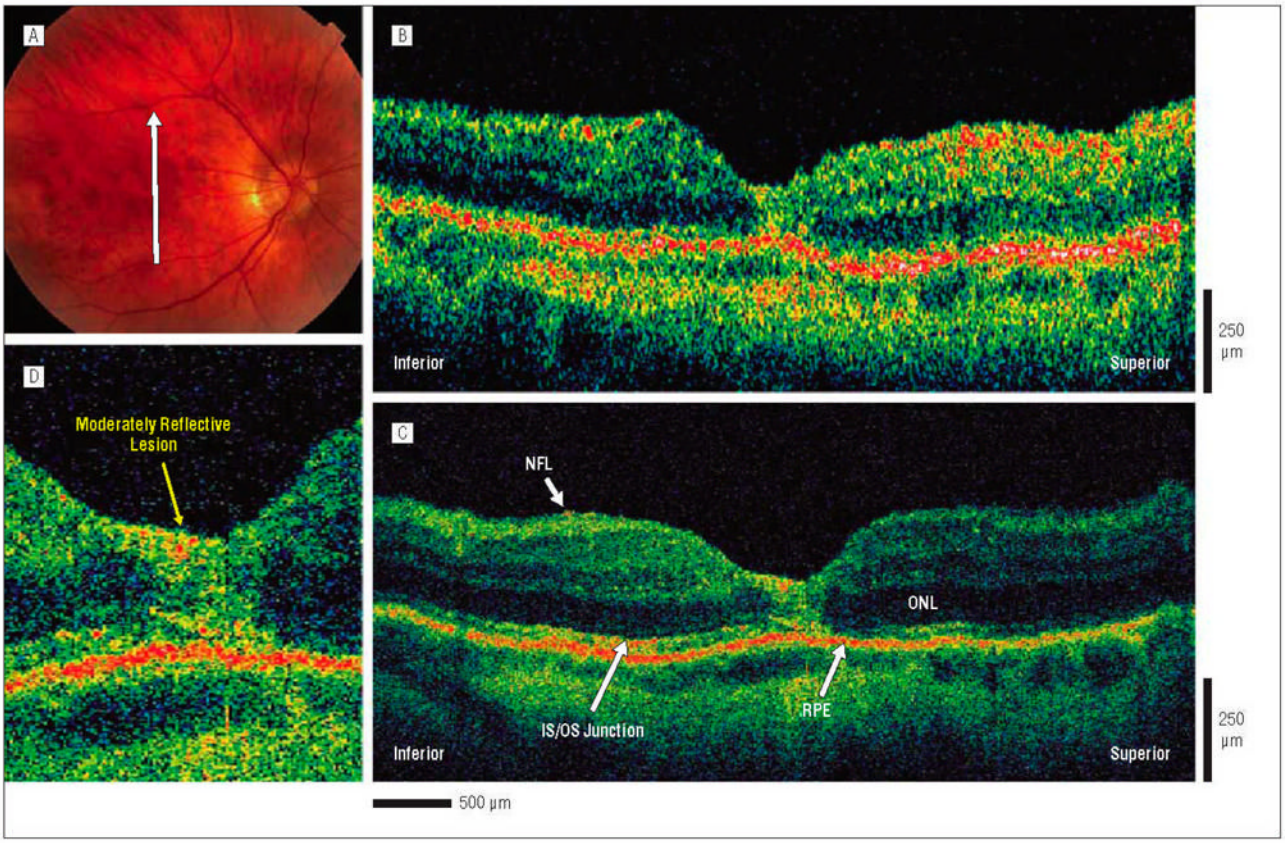

Figure 5.

Postoperative macular hole, 1 month after surgical repair. The patient is a 66-year-old man who underwent initial evaluation for a stage 2 macular hole in the right eye and had a preoperative visual acuity of 20/80. He underwent pars plana vitrectomy with internal limiting membrane peel and injection of 25% sulfur hexafluoride gas. One month later, the hole was flat and closed on results of examination, and visual acuity was 20/70. A, Fundus photograph shows the direction of optical coherence tomography (OCT) images. B, Standard-resolution OCT image acquired in the scan direction. The photoreceptor IS/OS junction appears disrupted, although it is difficult to distinguish this layer. C, Corresponding UHR-OCT image acquired in the scan direction. The intraretinal layers are better visualized in the UHR-OCT image, and it shows the large, moderately reflective foveal lesion replacing the normal foveal anatomy. D, Magnification (×2) of the UHR-OCT image. A large, moderately reflective lesion is replacing the normal foveal anatomy. All of the intraretinal layers of the fovea, including the photoreceptor inner and outer segments of the outer retina, appear to be involved. Abbreviations are described in the legend to Figure 1.

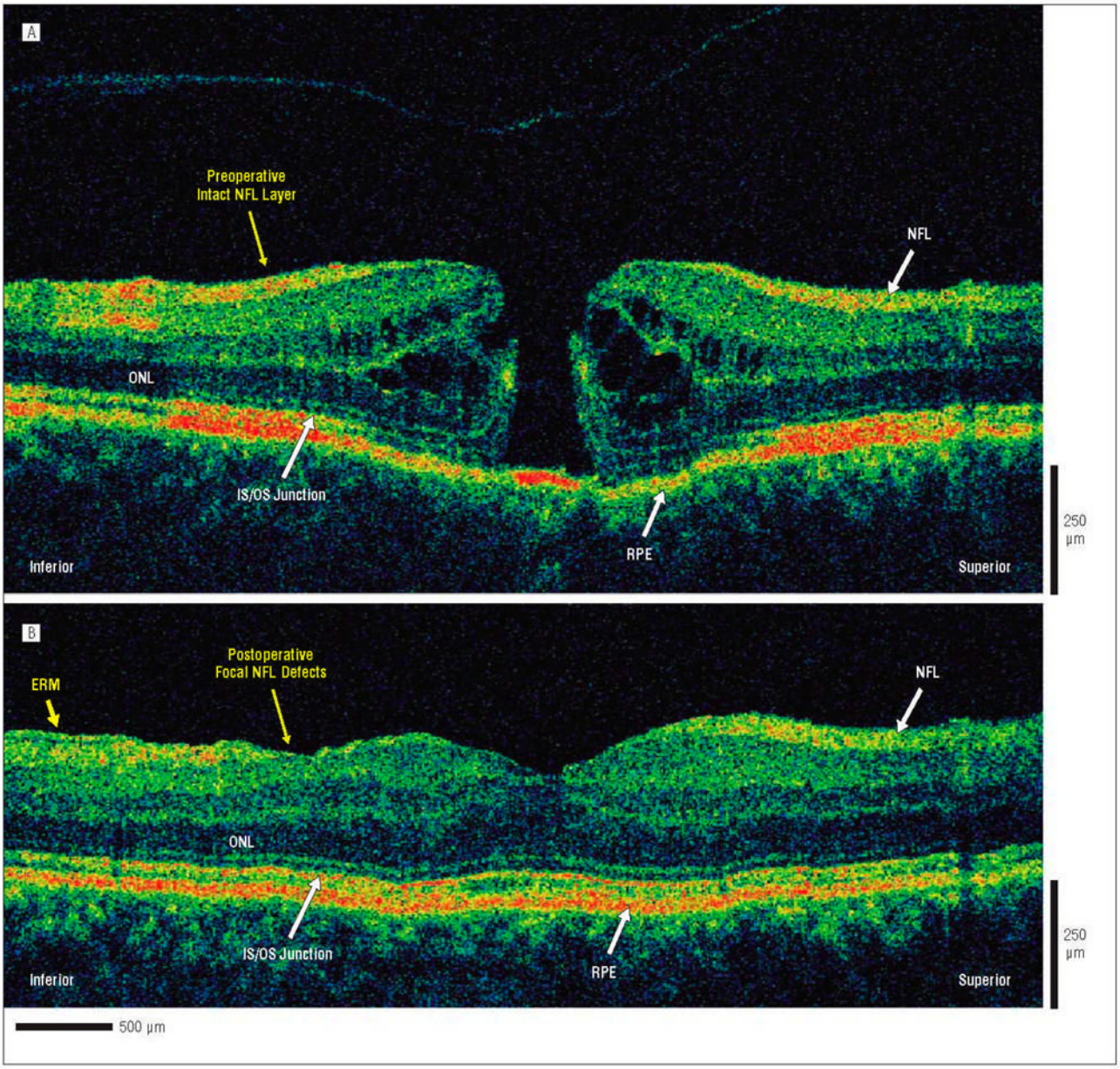

Figure 6.

Ultrahigh-resolution-optical coherence tomography (UHR-OCT) images of preoperative and postoperative macular hole. The patient is a 56-year-old woman who underwent initial evaluation for a stage 2 macular hole in the right eye and had a preoperative visual acuity of 20/60. She underwent pars plana vitrectomy with internal limiting membrane peel and injection of 25% sulfur hexafluoride gas. Five months later, the hole was flat and closed on results of examination, and visual acuity was 20/50. The UHR-OCT images were acquired across the macular in the inferior-superior direction. A, Preoperative UHR-OCT image acquired in the inferior-superior direction. A stage 2 full-thickness macular hole is clearly visualized. Nerve fiber layers (NFLs) inferior and superior to the hole appear to be intact and normal. B. Corresponding postoperative UHR-OCT image acquired in the inferior-superior direction. The hole appears to have been closed with the return of normal retinal anatomy. Focal defects in the NFL are apparent in the inferior portion of the image, whereas the NFL in the superior

portion of the image appears to be intact and normal. An epiretinal membrane (ERM) can be visualized at the edge of the scan adjacent to the NFL defect. Although no foveal photoreceptor abnormality is seen in this UHR-OCT image obtained in the inferior-superior direction (90°), another postoperative UHR-OCT image obtained at 30° (not shown) detected a hyporeflective disruption of the foveal photoreceptor IS/OS junction. Abbreviations are described in the legend to Figure 1.